



INSTITUT DE FRANCE  
Académie des sciences

# *Comptes Rendus*

---

## *Physique*

Romain Gautier, Armin Rajabzadeh, Melvyn Larranaga, Nicolas Combe, Frédéric Mompiau and Marc Legros

**Shear-coupled migration of grain boundaries: the key missing link in the mechanical behavior of small-grained metals?**


Volume 22, issue S3 (2021), p. 19-34

<<https://doi.org/10.5802/crphys.52>>

**Part of the Special Issue:** Plasticity and Solid State Physics

**Guest editors:** Samuel Forest (Mines ParisTech, Université PSL, CNRS, France) and David Rodney (Université Claude Bernard Lyon 1, France)

© Académie des sciences, Paris and the authors, 2021.  
*Some rights reserved.*

 This article is licensed under the  
CREATIVE COMMONS ATTRIBUTION 4.0 INTERNATIONAL LICENSE.  
<http://creativecommons.org/licenses/by/4.0/>



*Les Comptes Rendus. Physique sont membres du  
Centre Mersenne pour l'édition scientifique ouverte*  
[www.centre-mersenne.org](http://www.centre-mersenne.org)



---

Plasticity and Solid State Physics / *Plasticité et Physique des Solides*

# Shear-coupled migration of grain boundaries: the key missing link in the mechanical behavior of small-grained metals?

*Migration couplée au cisaillement des joints de grains :  
le chaînon manquant dans le comportement mécanique  
des métaux à petits grains ?*

Romain Gautier<sup>a, b</sup>, Armin Rajabzadeh<sup>a</sup>, Melvyn Larranaga<sup>a</sup>,  
Nicolas Combe<sup>a</sup>, Frédéric Momprou<sup>a</sup> and Marc Legros<sup>\*, a</sup>

<sup>a</sup> CEMES-CNRS, 29 rue J. Marvig 31055, Toulouse, France

<sup>b</sup> Institut Pprime - CNRS, 2 boulevard des Frères Lumière 86360,  
Chasseneuil-du-Poitou, France

*E-mails:* romain.gautier@cemes.fr (R. Gautier), armin.rajabzadeh@pwc.ca  
(A. Rajabzadeh), melvyn.larranaga@cemes.fr (M. Larranaga),  
nicolas.combe@cemes.fr (N. Combe), frederic.momprou@cemes.fr (F. Momprou),  
marc.legros@cemes.fr (M. Legros)

**Abstract.** Grain size reduction is a very efficient way to block dislocation movements and therefore create very strong metals and alloys. Not only grain boundaries are known obstacles for dislocations, but when reaching nanometer dimensions, crystallites usually become dislocation free, which imposes an additional constraint to develop plasticity. A recent effort to understand grain boundaries-based deformation mechanisms has therefore emerged. These mechanisms can be manifold, involving conservative and diffusive processes that are very poorly understood. A first approach consisting in downscaling mechanisms that are documented at large scale such as Coble creep, proved very limited. On the other hand, stress-assisted grain growth or shear-coupled grain boundary migration, that were recently observed in small-grained materials at room or low temperature may provide a crucial step to fully understand dislocation-less plasticity in nanocrystals. As this is a completely new field with many more degrees of freedom, a continuous research effort has to be carried out to link the mechanical properties of nanocrystals to these mechanisms specifically linked to grain boundaries.

**Résumé.** La réduction de la taille des grains est un moyen très efficace de bloquer les mouvements de dislocations et donc d'augmenter la résistance mécanique des métaux et alliages. Non seulement les joints de

---

\* Corresponding author.

grains sont des obstacles connus pour les dislocations, mais lorsqu'ils atteignent des dimensions nanométriques, les cristallites deviennent généralement vides de dislocations, ce qui impose une contrainte supplémentaire pour développer la plasticité. Comprendre les mécanismes de déformation basés sur les joints de grains est devenu un enjeu majeur de la métallurgie physique. Ces mécanismes peuvent être multiples, impliquant des processus conservatifs et diffusifs qui sont mal compris. Une première approche qui consiste à transposer aux petites dimensions des mécanismes documentés à grande échelle comme le fluage de Coble, s'est avérée très limitée. Au contraire, la croissance des grains assistée par la contrainte ou la migration des joints de grains couplée au cisaillement, récemment observées dans les matériaux à petits grains à température ambiante, peuvent fournir une clé pour comprendre pleinement la "plasticité sans dislocation" dans les nanocristaux. Comme il s'agit d'un domaine relativement nouveau avec beaucoup plus de degrés de liberté, un effort de recherche continu doit être mené pour relier les propriétés mécaniques des nanocristaux à ces processus de plasticité basés sur les joints de grains.

**Keywords.** Grain boundaries, Disconnections, plasticity, mechanical behavior.

**Funding.** This work has been financially supported by the Agence Nationale de la Recherche through the "Rodin" project, ANR-17-CE08-0007.

Available online 21st June 2021

## 1. Introduction

### 1.1. *Origin of hardening in metals*

As the main vector of plastic deformation in crystals, the mobility of dislocations directly influences the mechanical properties. This is why hardening a metal mainly consists in blocking or hindering dislocation movements. Among the many ways to do so, the oldest one lies in multiplying obstacles, often embodied by extrinsic atoms present in metallic alloys [1, 2]. Strain (or Taylor-) hardening is caused by the development of a dense dislocation microstructure where dislocations themselves become their own obstacles. The most prominent example of such hardening mechanism is fatigue where dislocations self-arrange in so-called "walls" that grow impermeable to further plasticity, delimiting "channels". As the channels become narrower, mobile dislocation are forced to curve tighter [3], requiring additional stress to maintain plastic deformation. Similar confinement-driven hardening is observed in Severe Plastic Deformation processes, that lead to the formation of dislocation cells, low- then high-angle grain boundaries (HAGB) upon increasing strain [4–6]. Such top-down methods usually manage to reduce the grain size to a few hundreds of nm, but going further down requires bottom-up methods such as physical or chemical deposition, crystallite condensation and agglomeration [7, 8]. In fact, the microstructure of pure metals becomes thermodynamically unstable when they contain too many grain boundaries, and grain growth or recrystallization is observed at room temperature [9–11].

### 1.2. *Mechanical behavior of nc-metals*

Reducing the grain size of a polycrystalline metal or alloy to increase their yield stress has been rationalized through the Hall-Petch relation that states that the yield stress of steels goes up as the inverse of the square root of the average grain size [12–14]. This empirical law has then been verified for a number of metals and alloys, mainly with fcc structures [15, 16]. But as with other systems where dislocations are confined in a given volume (thin films on substrates, pillars and nanowires [17]), the yield stress increase due to the path limitation of mobile dislocations ultimately saturates when entering the sub-micron or nanocrystalline regime [18]. In this so-called "Hall-Petch breakdown regime", plateaus or decrease of the yield stress have been reported [19].

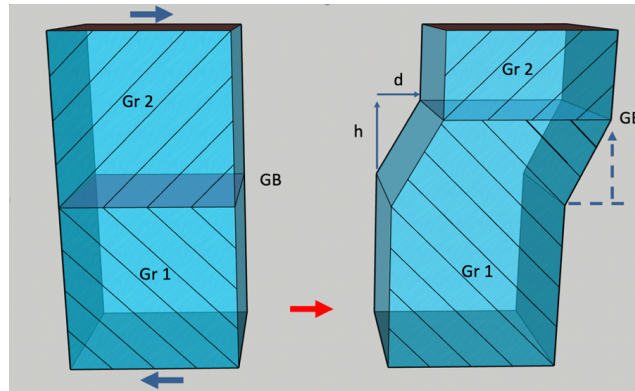


**Figure 1.** Principle of shear coupling grain boundary migration. Under shear (bold blue arrows), a GB migrates by a distance  $h$  from the position on the left figure to its position on the right figure. A shear ( $d$ ) occurs along the GB plane. The coupling factor defining the amplitude of the shear associated with this process is  $\beta = d/h$ .

In such nanocrystalline (nc-) materials, the proportion of atoms involved in grain boundaries (GB) can reach several percents, and the dislocation mean free path can be reduced to the grain size [20]. The plastic deformation of such nanocrystals would require the cooperative motion of several dislocations in most grains [21], which is practically impossible, especially when experimental observations return an intragranular dislocation content nearing zero [7]. As a result, nc-metals generally show very low to almost no ductility [7]. However, in some occurrences, nanocrystalline metals can exhibit significant ductility [22,23], and many experiments or simulations [24,25] have pointed to “GB-based plasticity” to explain it. This generic appellation encompasses many possible mechanisms, going from GB sliding to grain rotation [26]. These mechanisms would also be responsible for the Hall–Petch breakdown regime, and could be based on diffusion [27] or conservative processes [28]. Direct observations of these GB-based mechanisms are very difficult to obtain for reasons that will be developed later, but early reports of their occurrences in the mid 2000’s eventually made headlines [29] or sparked controversy [30].

### 1.3. Shear-coupled grain boundary migration

Among all the GB-based plasticity processes, the shear-coupled GB migration (SCGBM) particularly captured attention because it may produce significant shear, it is a conservative mechanism, and also because it probably relates to another extensively observed phenomenon in nc-metals : shear-assisted grain growth [31–34]. This later mechanism is clearly different from traditional recrystallization or grain growth as both these microstructural changes occur without shape change. The mechanism of shear-coupled grain boundary migration is not as intuitively understandable as for dislocation shear. Figure 1 illustrates how it occurs phenomenologically, and how it is measured through the quantity  $\beta$ , that is called the coupling factor: under a shear stress, the grain boundary (GB) separating grain 1 and grain 2 moves along its normal (either upwards or downwards). This migration over a distance  $h$  is accompanied by a shear displacement  $d$ .  $\beta$ , the coupling factor, is the ratio of  $d$  over  $h$ .

Shear-coupled grain boundary migration was first theorized by Read and Shockley who considered low-angle grain boundaries as arrays of perfect lattice dislocations. These dislocations could simultaneously move by application of an external shear stress, resulting in the migration

of the low-angle grain boundary [35]. Experimental observations came shortly after in zinc bi-crystals [36, 37]. The topological dislocation content of any grain boundary can be obtained from the Frank–Bilby equation [38] and this served as the basis of the Cahn, Mishin, Suzuki, and Taylor (CMST) model which extended the low-angle grain boundary model from Read and Shockley to any [001] tilt boundary in fcc structures [39]. It should be noted that a similar model for NaCl-type cubic structures was published by Guillope and Poirier in 1980 [28]. Logically, this conservative model predicts that the larger the misorientation, the larger the shear carried by a given GB (modulo the 90° symmetry of this specific tilt axis). Experiments carried out at medium-to-elevated temperatures (300-400°C) on Al bi-crystals tended to support this model [40] (Figure 2), although some scatter in the results existed and some of them were discarded when only segments of the GB coupled for example [41].

This model, appealing by its simplicity, suffers however, from several drawbacks:

- The dislocation content of high-angle grain boundaries is only virtual as their core overlap once a 10-15° misorientation is surpassed so that their existence as single defects when the boundary misorientation is high becomes impossible.
- The model only applies to a specific type of boundaries, and its extension to general boundaries such as the ones present in real crystals may be facing limitations. The first one being that twist boundaries shouldn't be able to shear-migration couple.
- The main limitation is that only perfect lattice dislocations are considered as intrinsic GB defects while it has been shown that dislocations with smaller Burgers vectors (DSC - Displacement Symmetry Conserving - see discussion section) exist and might be activated at lower energy cost (owing to their shorter Burgers vector).
- Finally, if one only considers GB misorientation, the coupling factor predicted by the CMST model is often very high and incompatible with experimental observations in polycrystals.

In the Cahn, Mishin, Suzuki, and Taylor (CMST) model [39], as the GB misorientation is a direct function of its virtual dislocation content,  $\beta$  goes up with the GB misorientation, and coupling factors as high as 50 to 100% are theoretically possible for symmetric tilt boundaries in the range of 30° to 40° misorientations. Such amounts, seldom seen in specific bicrystal experiments [40] and simulations [42] have never been reported in polycrystals. In early experiments on ultra fine Al grains [43], it was found that the shear produced by mobile grain boundaries seems poorly connected to their misorientation. Molecular dynamics-based simulations [44] and paper cuts-based topological calculations [45] revealed that the coupling factor associated with a given grain boundary could be manifold, and in particular that much lower coupling factors could be found for symmetric <001> GBs. In the following, we will show how complementary approaches (experimental and computational) are used to quantify shear-coupled grain boundary migration in small-grain polycrystals and to unveil the atomic processes at play when the mechanism is active.

## 2. Methods and results

### 2.1. *In-situ TEM*

Ultra Fine Grain (UFG) pure and alloyed (1-3wt% Mg) aluminum was processed by high pressure torsion in ESI, Leoben, resulting in  $\varnothing$ 25 mm, 4mm thick discs with an average grain size of 160 nm (Al1%Mg) and 110 nm (Al3%Mg). Alloying Al with Mg allows to stabilize a small grain size as pure UFG Al experiences grain growth even at room temperature. 1 x 3 x.5 mm rectangles are then cut with an electro-discharge machine and mechanically polished down to 20-50  $\mu$ m thickness using SiC grinding papers of diminishing grids. A circular electron-transparent zone

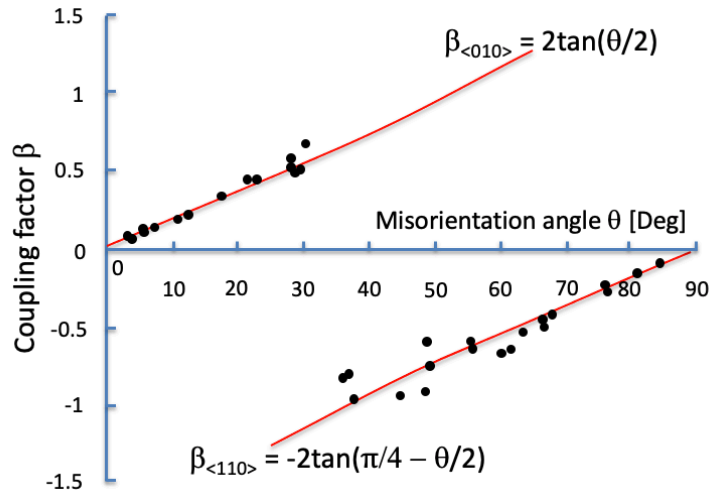


**Figure 2.** Coupling factor as a function of misorientation for [100] coherent tilt boundaries in fcc metal. The two red curves  $\beta = 2 \tan(\theta/2)$  and  $\beta = 2 \tan(\pi/4 - \theta/2)$  are derived from the CMST model [39]. The dots are experimental points from bicrystals experiments by Gorkaya *et al.* [40].

is then created in the middle of these rectangles using a 33% nitric acid methanol solution in a Tenupol electro-polishing unit at  $T = -10^\circ\text{C}$ . The in-situ TEM straining experiments start by gluing the samples on copper straining grids using epoxy glue or zirconia-based cement. A first step consists in initiating a micro-crack at room temperature. This is followed by a mild annealing at  $220^\circ\text{C}$  for 5 minutes inside the TEM on a home-made heating-straining holder to remove most of intra-granular dislocations. ASTAR-ACOM (Automatic Crystallographic Orientation Mapping) is then performed to assess the new average grain size (270 nm for Al1%Mg and 145 nm for Al3%Mg) and in the specific zone ahead of the crack tip on a CM20 FEG TEM. The reason UFG Al is chosen over nc-Al is that  $e^-$  transparent regions are typically below 400 nm thickness in these TEM foils. Having grain sizes much lower than that (typically in the 10-50 nm range) would cause multiple grains to diffract simultaneously, hampering their indexation. Grain-boundary migrations are monitored during more extensive in-situ straining experiments carried out on the CEMES-custom-made high temperature straining holder fitting a JEOL 2010 TEM. Once several SCGBM events are recorded, the experiment is stopped and the sample is returned to the CM20 FEG TEM to perform a post-straining ASTAR-ACOM crystal orientation map. The shear induced by grain boundary migration is assessed through digital image correlation analysis (open source Open CV software [46]) from images captured from videos recorded through a MegaView III CCD camera (SIS-Olympus) side-mounted on the JEOL 2010 TEM.

## 2.2. In-situ TEM results

Figure 3 is an example of the results obtained using the procedure that has been elaborated at CEMES to quantify the coupling factor on known grain boundaries in UFG metals. Figures 3 (a), (b) are video stills extracted from a video sequence where a grain boundary migrates under stress

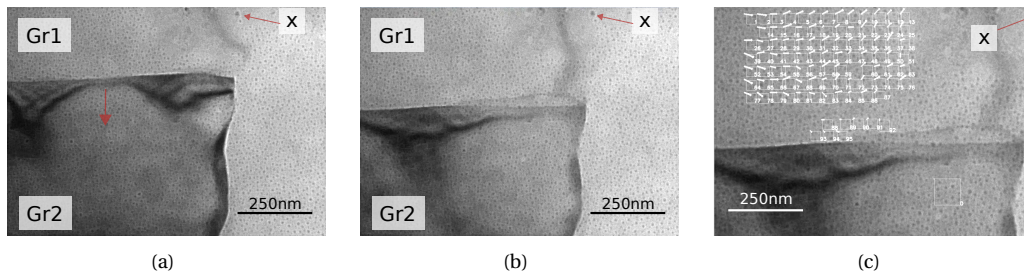


**Figure 3.** Shear-coupled grain boundary migration measurement on a migrating grain during an in-situ TEM straining experiment at 490 K. (a) Position of the GB before migration. (b) After 52 s, the GB moves upwards (X represents a fixed point in the sample between both video stills). (c) The carbon contamination accumulating during the initial sample heating serves as markers for DIC. Points in each white square are compared to their initial position prior to GB migration. Cross-correlation defines the direction and amplitude of the shear. (arrows are 4x longer than the actual shear displacement).

(tensile stress, vertical on the pictures). The stress state is not known here, as a slowly opening crack tip is located a few microns away (upper right corner) from the mobile GB. An evaluation of the stress was made from a single spiral source operating near a crack-tip (zone similar to those where SCGBM occurs). The line tension approximation  $\tau = \mu b / 2R$ , where  $R$  is the radius of curvature of the dislocation and  $\mu$  the shear modulus of Al at 400 K (22 GPa) returned a resolved shear stress  $\tau = 19 \pm 3$  MPa.

As in the example above, most of the GB movements are usually smooth and proceed by alternating periods of activity and usually longer periods where they are immobile. Collapsing of smaller grains usually accelerates until their complete annihilation, which suggests that surface tension effects take over when the GB size goes below 50-100 nm. In examples such as in Figure 3, flat segments of GB are moving, excluding capillarity effects and attesting of the shear-coupling mechanism.

Similar GB movements have been observed regularly in our in-situ TEM experiments even if they are complicated to fully capture: GB migration under stress occurs among groups of grains and may cease after a few seconds to resume in another location. These movements are then limited in time and space and, to date, impossible to predict. The migration of GBs is almost never jerky, but may proceed by successive rapid movements of segments while others stay put. Speeds on the order of 1-2 nm/s are regularly observed. To analyze the shear produced by the migration, simple digital image correlation (DIC) using a custom script is performed on two sets of about 30 square zones (white squares in Figure 3 (c) located ahead and aside from the moving GB. Each square zone contains several markers (surface contamination) and the produced shear is the average value returned by the square box displacement in the direction parallel to the GB plane divided by the migration distance. In this case, this yields 3% in average ( $\pm 1\%$ ). This average is obtained after measuring shear migration couples at 29, 57 and 87 nm migrations. At each of these steps, the shear was 0.8, 0.8 and 3 nm, respectively. Despite the DIC returning a sub-pixel resolution, we cannot claim a resolution better than 1 nm, which may explain why the first two measurements, being in the error bar of the technique, give the same value. Moreover, the marker displacements are not everywhere parallel to the GB plane, which indicates that the overall strain field resulting from deformation in neighboring grains is more complicated than a simple shear. Overall, these small values are however typical of our experiments where coupling factors are low in most cases: a significant migration is therefore needed to obtain measurable coupling factors.

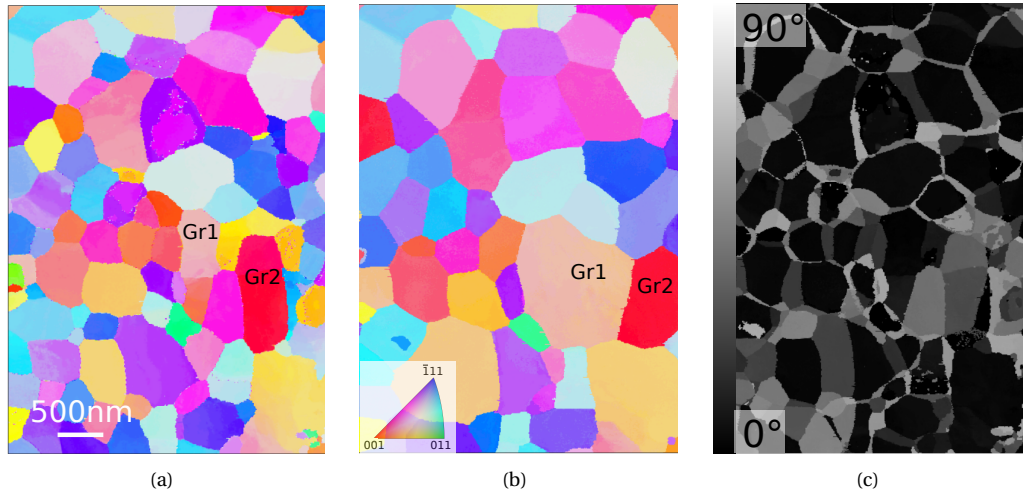


**Figure 4.** Stress-assisted grain growth in Al3%Mg at 220°C. (a), (b) ASTAR-ACOM crystallography mapping of a zone ahead of a propagating crack tip before (a) and after (b) stress-induced GB migration. In (c), map of the minimum misorientation angle between the two maps (a)-(b) corrected from rigid-body rotation due to crack propagation. The black pixels represent grain interiors that haven't changed during grain growth (55% of the total surface-see text for details).

Referring to the misorientation map of Figure 4 (c), the minimal misorientation between grains 1 and 2 is 26.9°, around a  $[450 -240 162]$  (close to  $[3-21]$ ) axis. According to the CMST model,  $\beta$  should be equal to 47% if the (100) mode is activated or 122% for the (110) mode and considering a pure tilt GB. The orientation maps seen in Figures 4 (a)-(b) attest that a massive grain growth is taking place under stress. This is visible in Figure 4 (c), where only zones that are not affected by GB migrations are in black. In this figure,  $7.85 \mu\text{m}^2$  out of the  $17.44 \mu\text{m}^2$  (45%) of the map are affected by grain migration. This surface change corresponds to a grain size increase of 48%, significantly larger than the one only obtained by annealing (110 to 145 nm), corresponding to a 32% increase for the same temperature. To account for the rigid-body rotation due to the crack propagation (not seen on the pictures) and the subsequent tilt affecting the TEM sample, this average rotation is subtracted to the orientations in the map of Figure 4 (c). This map represents the minimum misorientation angle between the two maps of Figures 4 (a), (c), corrected from rigid-body rotation due to nearby crack propagation and obtained using a custom script [47]. One can then see that some grains are growing at the expense of smaller grains. The sequence seen in Figures 4 (a)-(b) occurs between grains Gr1 and Gr2 labeled in Figure 3 (b) (after the growth of grain 1 towards grain 2 across the yellow grain in between - Figure 3 (a)).

Although seldom evidenced, moving lines bound to migrating or sliding GBs can be seen (Figure 5) when imaging conditions are favorable. GBs have to be sufficiently inclined from their edge-on position for instance. In this sequence, these lines were observed to steadily move from a surface defect pointed by the red arrow in Figure 5 (a) (towards the upper left triple junction TJ), a second TJ is also visible on the lower right side of the figure). Since these linear defects are strictly attached to the GB and because they show a dislocation-like behavior, we think they are disconnections (see Figure 6, Figure 8), although we cannot attest their step character in this case (wrong orientation of the foil and insufficient resolution). No stress concentration can clearly be seen at triple junctions, but many pieces of evidence show that this specific



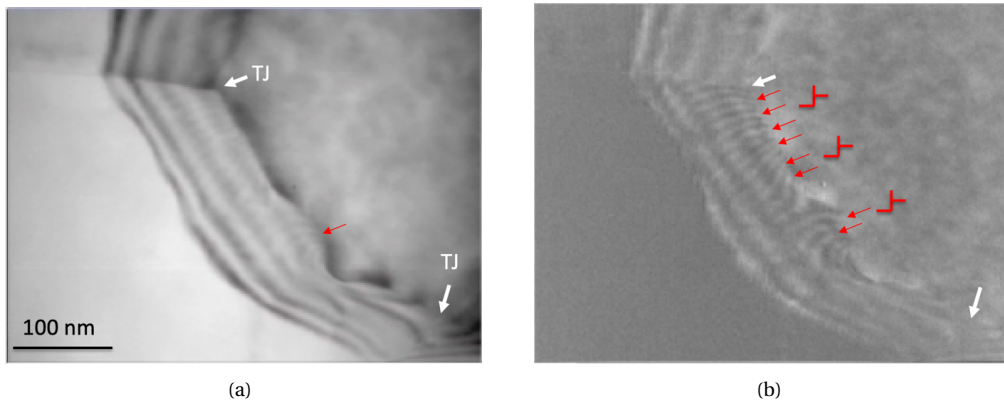


**Figure 5.** Video frame captured during an in-situ TEM deformation experiment of an UFG pure Al at RT. (a) Disconnections with very faint contrast move from a surface defect (below the small red arrow in a) to a triple junction (TJ, upper left). (b) Two images separated by 7.5 s are subtracted to enhance the contrast of the moving disconnections (┘┘). Red arrows point to some of them.

location of polycrystals serve both as source and sink for disconnections. The difficulty to obtain strong contrasts of disconnections is probably due to their position between two diffracting/non-diffracting grains, and also to the fact that many of them possess a shorter Burgers vector (DSC dislocations) compared to lattice dislocations. As a result the distortion of the crystal around these defects is limited and their diffraction contrast faint. In most of our observations, trains of disconnections move along segments of grain boundaries and seem to have similar Burgers vector as their contrast, even light, is similar (Figure 5).

### 2.3. Simulation: Nudge Elastic Band (NEB) method

In the Molecular Dynamics simulations carried out by Mishin and co workers, the shear coupled migration is observed to occur by successive and sudden jumps of the GB [39]. We have investigated one of the systems they studied: a copper bicrystal containing a planar symmetric coincident  $\Sigma 13$  (320) tilt grain boundary, with a misorientation of  $67.38^\circ$  around a [001] rotation axis (Figure 6).

We use an EAM Cu potential [48], and the LAMMPS simulation package [49]. Performing a shear loading until GB migration and then an unloading, we determined two stable states of the bicrystal corresponding to configurations before and after the first migration of the GB (blue points  $c_i$  and  $c_f$  respectively, in Figure 6(c)), for a given position of the slabs (or a given strain). In order to determine the Minimum Energy Path (MEP) between the  $c_i$  and  $c_f$  configurations i.e. the lowest energy curve that connects them in the energy landscape, we performed NEB calculations: for a  $N$  atoms system, an extended phase space (dimension  $3Nm$ ) is defined using intermediate configurations of the system (or replicas) as  $\mathbf{R}_i$  atomic arrangements ( $3N$  coordinates),  $i = (0, \dots, m-1)$ ,  $\mathbf{R}_0$  being the initial state before the GB jump (configuration  $c_i$ ) and  $\mathbf{R}_{m-1}$  the final one after the jump (configuration  $c_f$ ). Harmonic potentials couple replica in order to form an elastic band and atoms in a replica interact through the EAM potential. The NEB method applies a judicious dynamics to this system in order to drive it to the MEP (more details can be found in [50, 51]). Figure 7 shows such a path as a function of a reaction coordinate (RC). The RC is here

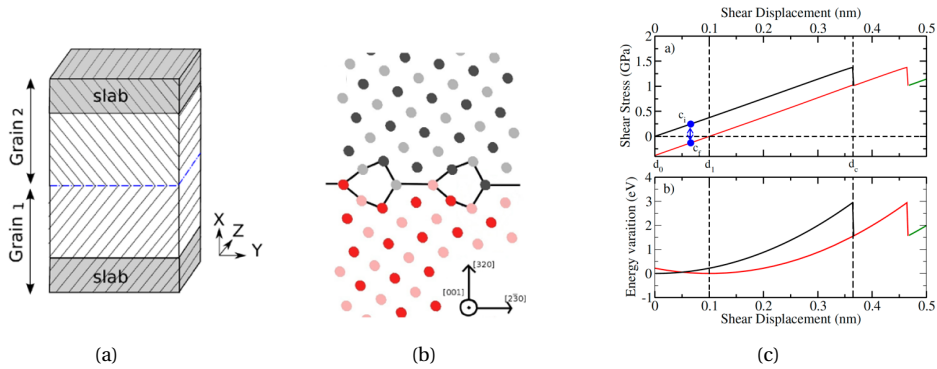


**Figure 6.** (a) Configuration of the simulation box containing a planar symmetric coincident  $\Sigma 13$  (320) tilt grain boundary, with a misorientation of  $67.38^\circ$  around a [001] rotation axis. The shear is applied horizontally on atoms contained in both slabs (1.5 nm thick) on top and bottom of the bicrystal. (b) Equilibrium atomic configuration of the GB, showing 2 structural units (“kite” shape). Black (red) and grey (pink) atoms are on different  $z$  coordinates. (c) Shear and elastic energy as a function of the slab displacement at 0 K. The black curve represents the elastic loading, followed by a GB jump. The red curve corresponds to the atomic configuration of the simulation box after the migration of the GB (including its unloading).

defined as the cumulative distance (normalized by the total cumulative distance) between adjacent replicas in the configuration space of dimension  $3N$ . In Figure 7, the cell size is  $10.3 \times 6.5 \times 1.4$  nm ( $X \times Y \times Z$ ), and the cell contains 12 structural units such as the ones in Figure 6.

Figure 7 shows multiple local minima which atomic configurations are displayed in the figure. The SCGBM mechanism occurs through the nucleation (from states (a) to (b) in Figure 7), motion (from states b to j in Figure 7) and recombination (from states j to k in Figure 7) of GB steps. We have identified these GB steps as disconnections by performing a Burgers circuit analysis around them. The two GB steps have opposite Burgers vectors and step height: respectively  $b=0.1$  nm and  $h=0.25$  nm (see also Figure 8 for disconnection description). At the end of the reaction ( $RC=1$ ), the grain boundary moved down by the step height  $h$  and the bicrystal is sheared by an amount of  $b=0.1$  nm. The coupling factor is directly derived from this process as  $\beta = b/h = 0.4$ . The nucleation and propagation of a disconnection along a GB constitute therefore the basic mechanism of the shear-coupled GB migration. This migration can then be seen as a continuous process, at variance of the stick-slip motion previously considered. Finally, the process also gives physical sense to the coupling factor, that is simply the Burgers vector divided by the step height of the moving disconnections.

### 3. Discussion

To fully assess for the deformation mechanisms at play in nanocrystalline metals and alloys, GB-based plasticity has to be better understood. Consistently with previous observations, we have shown that stress-assisted grain growth occurs through the migration of the grain boundaries, and that this migration can occur without involving lattice dislocations [52]. In the example reported here (Figure 3), it should be noted, that at variance from recrystallization processes, no intragranular dislocations are involved, and that the moving GB is almost flat, which eliminates the elastic energy gradient and curvature-driven migration that are often invoked for such

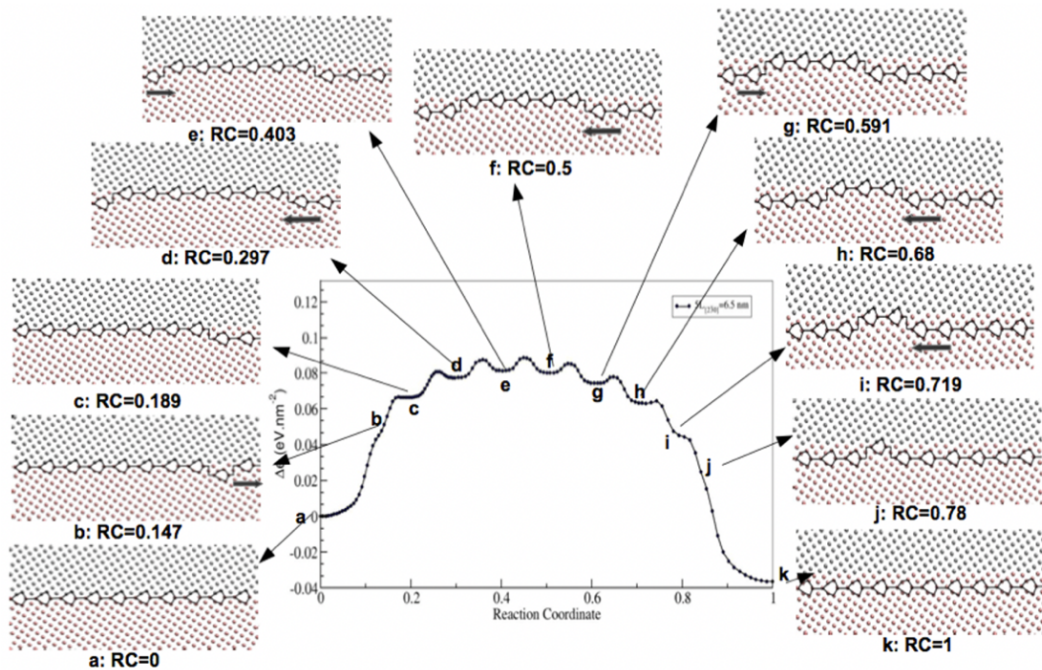


**Figure 7.** Energy landscape during the migration of a simulated perfect coincident  $\Sigma 13$  (320) tilt GB at zero K under stress in an artificial Cu bicrystal containing 12 structural units (after [50]). (See text for details).

GB rearrangements. As in previous studies [53–55], we report small shear migration coupling factors, on the order of a few percents, a quantity that is in line with the applied strain. Also consistently with similar studies in nanocrystalline Cu, all the types of GB migrate, irrelevant to the misorientation they carry [56–58]. In all these studies, no specific stress concentration that could result from incompatible GB processes are reported. This supports the possibility of GBs with various misorientations to adopt different coupling factors so that grain growth happening through SCGBM does not create low shear/high shear zones. One common belief or approach in GB-based plasticity is that moving GBs would act similarly to dislocations, but at a larger scale and dimension. The corollary of this approach is to consider the defining parameters of the GB, and especially the misorientation as an intrinsic value from which the coupling factor will depend [59]. Low coupling factors would be the result of a judicious combination of two coupling modes [60].

A more recent approach, that we would like to promote here, considers each grain boundary as a network with its own translations and symmetries that differ from the crystal lattices of its two adjacent grains. In particular, this “coincident site lattice” (CSL) possesses translational invariants (and thus possible GB Burgers vectors) that have a much smaller amplitude than those of the adjacent grains. These possible shear vectors are called DSC, for “displacement shift complete” or “displacement symmetry conserving” [61]. When a perfect dislocation reacts with a GB, a dissociation into these smaller Burgers vectors is energetically favorable [62]. Similarly, if these shear vectors are involved in the SCGBM process instead of perfect grain lattice Burgers vectors, they will lead to smaller shears and thus smaller coupling factors (for a given step height). The main contribution of these DSC vectors is to provide many more combinations with interplanar distances (possible steps) and therefore a much larger number of coupling factors for a given

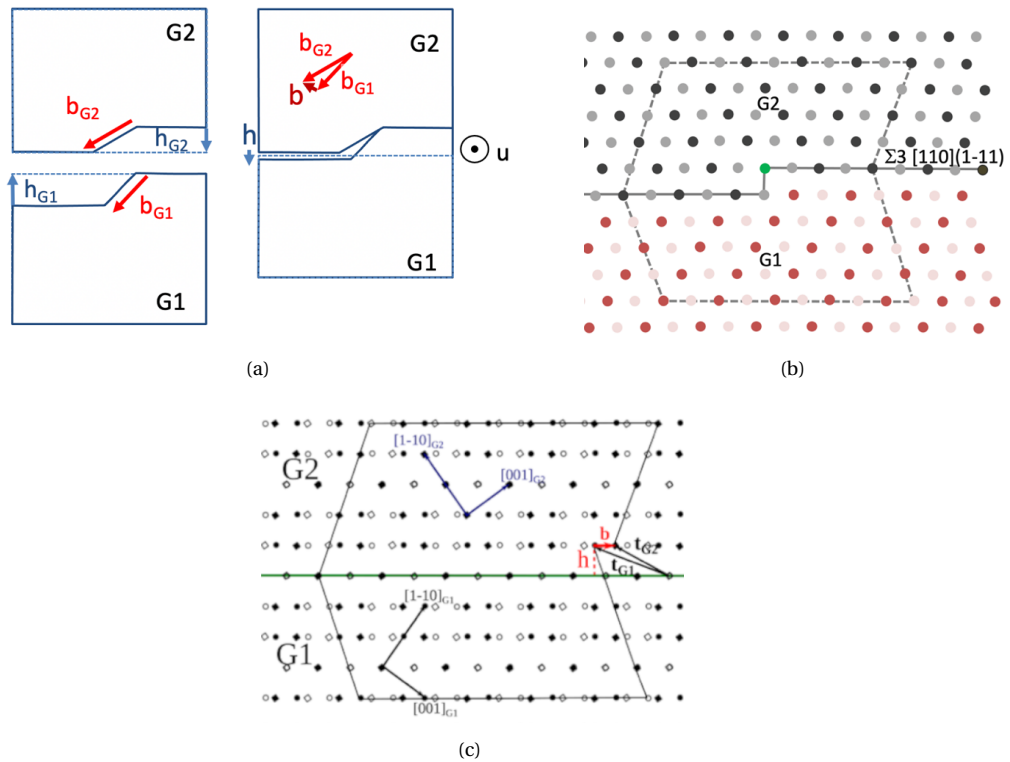


**Figure 8.** (a) Topological construction of a disconnection joining two incompatible stepped grains G1 and G2.  $b_{G1}$  (resp.  $b_{G2}$ ) and  $h_{G1}$  (resp.  $h_{G2}$ ) are Burgers vector and step belonging to grain 1 (resp. grain 2). The resulting disconnection has a Burgers vector  $b = b_{G1} - b_{G2}$  and a step height  $h = (1/2)(h_{G1} + h_{G2})$ . (b) Example of a disconnection (located on the green atomic row) in a  $\Sigma 3[110](1\bar{1}1)$  grain boundary in a fcc crystal. The disconnection is identified using a Burgers circuit between grain 1 and grain 2 and reported in the dichromatic pattern in (c). Here, the disconnection is one interplane distance high with  $b = 1/6[1\bar{1}2]$  (in G1). In (b), the atoms in each grain are colored according to their z coordinates.

GB, compared to models where deformation carriers are limited to intrinsic dislocations. It explains why this diversity of coupling factor has been found in purely topological models [45] and extensive MD simulations [44]. In fact, the CMST model may provide an upper bound for the various coupling factors found in these other models, although the SMIG model [45] has no energetic considerations and is therefore not imposing a maximum  $\beta$ . The defect combining one dislocation (perfect or DSC) and a step is called a disconnection (Figure 8) [63]. A disconnection is specific to a GB and cannot escape from it unless it reacts to give rise to a regular lattice dislocation..

Inversely, lattice dislocations may enter GBs and decompose in several disconnections as their Burgers vector can be significantly smaller. Aside from diffusive process [64], lattice dislocations decomposing into disconnections may accelerate their absorption by GBs [65]. This explains in part why most real grain boundaries in materials contain disconnections. More generally, real GBs are rarely symmetric nor flat, nor do they have a pure tilt or pure twist character, and even without preliminary deformation, they contain disconnections of various characters [53]. This

defect has been known for decades in phase transformation and twinning [66–69], but has only recently been considered as the basic brick of shear-coupled GB migration [70–72], in metals with bcc and hcp structures too [73, 74]. One reason for this late acceptance is that the observation of moving disconnections is complicated experimentally, as in-situ TEM is almost the only way to do it [75] and that many atomistic simulations considered perfect GBs where the disconnection nucleation step overshadows the other mechanisms such as their propagation. Disconnections moving concomitantly to GBs in polycrystals have been seldom observed [76], as the obtention of a good contrast to image disconnections moving at an interface between two grains requires specific orientation conditions [77]. The coupling factor of a given GB would therefore not be the result of its macroscopic features (misorientation, habit plane), but its atom-scaled content, the disconnections. As many different types of disconnections can populate a given GB, the resulting  $\beta$  will be a result of the migration of these defects. Forecasting the behavior of a given GB would then require to know its disconnection content, which is probably extremely complicated to assess because of the number of possible combinations of diverse defects that would concur to the many degrees of freedom of a GB segment.

Such gap between disconnection-containing GBs in real materials and those used in atomistic simulations that are often perfect and separating only two grains (bicrystals) may explain why the observed coupling factors (low) differ from the simulated ones (high). In fact, atomistic simulations of real GBs are only beginning, addressing the possible influence of defects present prior to deformation such as vacancies [78] or immobile disconnections [79]. A second reason for the current mismatch between the observed and simulated coupling factors may be the complex stress tensor acting locally on real GBs in small-grained metals whereas atomistic simulations involve perfectly defined and often homogenous stress states [80]. These two factors may explain why many more disconnections could be activated in real metals at lower stresses and coupling factors while the nucleation step and strictly imposed strain directions favor a given disconnection that may have a large coupling factor in simulations.

Stress discrepancies are frequently observed between experimental and simulated plasticity studies [81], and the same goes for the SCGBM: the stress required to activate this mechanism remains poorly known. Atomistic simulations suggest levels of stress to move a perfect GB in bicrystals over 1 GPa in Al at 0 K [70] or in Cu at 400 K [39]. When defects are artificially introduced into these virtual GBs, the stress threshold to nucleate the first moving disconnection may be significantly lowered (about a factor 2 in [79]), but remains very high, especially when compared to experimental values. For instance, the Aachen team, specialized in Al bicrystals, was able to trigger SCGBM (generally done around 500-600 K) typically below 1 MPa [82]. This is more than 3 orders of magnitude lower, and it is arguable that the temperature and strain rate differences between virtual and actual experiments may not explain the whole story. In the polycrystal experiments reported here, there is no instrumented holder at play, so local stress levels can only be approximated using curved dislocations that are rarely observed as we take care of eliminating most of them prior to test the UFG samples. From a single spiral source operating near an opening crack-tip (zone similar to those where SCGBM occurs), we have determined that the plastic deformation occurred at a resolved shear stress of about 19 MPa, corresponding to an applied tensile stress of nearly 250 MPa if we consider the low (0.07) apparent Schmid factor, calculated in our case from the macroscopic tensile axis. This probably overestimates the applied stress as the stress tensor near a crack tip and close to grain boundaries may be strongly affected. Nonetheless, this stress value is in the order of what is found for UFG commercially pure Al at room temperature [83]. In other UFG / nanocrystalline metals studies, threshold values of 250-300 MPa have been reported at room temperature [58] (although it is not clear if a real plastic regime has been reached). More divergent values (between 100 and 400 MPa) have also been published for similar films, also at RT, with a strong effect on the grain size [23]. In this

later work, a clear GB-based plastic deformation was however observed slightly below 200 MPa. This very large range of stresses needed to trigger SCGBM, and the strong effect of temperature and grain size suggest that the mechanism is thermally activated. The temperature increase may be compensated by smaller grain size, which also suggest that diffusion is important, although we haven't considered it here, as disconnection mechanisms (glide) are conservative. The importance of diffusion was appreciable in the fact that triple junctions were observed to be both sources and sinks for disconnections [47, 76]. As diffusion and temperature directly influence the steps fluctuation in GBs [71], they must strongly influence the mobility of the GBs, but probably not their coupling with shear.

#### 4. Conclusion

In absence of dislocations, a mechanism called shear-coupled grain boundary migration (SCGBM) seems the most capable to alleviate for plasticity in nanocrystalline and small-grained metals. Current models and many simulations suggest that the coupling factor (shear over migration distance) depends directly on the misorientation carried by a given GB, and as such reaches values on the order of tens of percents. In-situ TEM experiments where migrating GBs under stress have been monitored and quantified suggest that the coupling factor  $\beta$  is generally close to a few percents, typically the amount of total deformation reached during the tests. No stress concentrations resulting from GBs migrating with very different  $\beta$  were observed. Convergent experiments (real and computed) point to disconnections as the basic brick of GB migration, which have very fundamental consequences: as a defect that possesses a step and dislocation character, each disconnection produces its own coupling factor. The coupling factor of a GB is the net sum of the shears and step heights carried by its operating disconnections, which, in turn implies that a given GB may have different coupling factors. In short, the coupling factor of a GB is not a unique function of its misorientation [84]. More generally, it may be foreseen that the GB properties such as its mobility or coupling factor are not intrinsic, but depend on the properties of its defects, namely the disconnections. The density of these defects, provided they are not all geometrically necessary along a finite length of GB, may also affect its energy. A key step in the coming years to understand the plastic behavior of small-grained metals is therefore to completely incorporate the disconnections into the problem. This defect is also probably a part of the solution to predict the mechanical behavior of this class of material as disconnections and dislocations share the same formalism. GB migration, but also GB transmission could be seen as a disconnection/dislocation problem.

#### References

- [1] R. W. Cahn, P. Haasen, *Physical Metallurgy*, 4th ed., Elsevier, 1996, 2740 pages.
- [2] D. Laughlin, K. Hono, *Physical Metallurgy*, 5th ed., Elsevier, 2014.
- [3] M. Legros, O. Ferry, F. Houdellier, A. Jacques, A. George, "Fatigue of single crystalline silicon: Mechanical behaviour and TEM observations", *Materials Science and Engineering: A* **483-484** (2008), p. 353-364.
- [4] M. Isik, M. Niinomi, H. Liu, K. Cho, M. Nakai, Z. Horita, S. Sato, T. Narushima, H. Yilmazer, M. Nagasako, "Grain Refinement Mechanism and Evolution of Dislocation Structure of Co-Cr-Mo Alloy Subjected to High-Pressure Torsion", *Materials Transactions* **57** (2016), no. 7, p. 1109-1118.
- [5] M.-p. Liu, T.-h. Jiang, X.-f. Xie, Q. Liu, X.-f. Li, H. J. Roven, "Microstructure evolution and dislocation configurations in nanostructured Al-Mg alloys processed by high pressure torsion", *Transactions of Nonferrous Metals Society of China* **24** (2014), no. 12, p. 3848-3857.
- [6] S. Scheriau, R. Pippan, "Influence of grain size on orientation changes during plastic deformation", *Materials Science and Engineering: A* **493** (2008), no. 1-2, p. 48-52.
- [7] M. Legros, B. R. Elliott, M. N. Rittner, J. R. Weertman, K. J. Hemker, "Microsample tensile testing of nanocrystalline metals", *Philosophical Magazine A* **80** (2000), no. 4, p. 1017-1026.

- [8] M. A. Meyers, A. Mishra, D. J. Benson, "Mechanical properties of nanocrystalline materials", *Progress in Materials Science* **51** (2006), no. 4, p. 427-556.
- [9] J. F. Humphreys, M. Hatherly, *Recrystallization and Related Annealing Phenomena*, Elsevier, 2012.
- [10] M. Ames, J. Markmann, R. Karos, A. Michels, A. Tschöpe, R. Birringer, "Unraveling the nature of room temperature grain growth in nanocrystalline materials", *Acta Materialia* **56** (2008), no. 16, p. 4255-266.
- [11] J. A. Haber, W. E. Buhro, "Kinetic Instability of Nanocrystalline Aluminum Prepared by Chemical Synthesis; Facile Room-Temperature Grain Growth", *Journal of the American Chemical Society* **120** (1998), no. 42, p. 10847-10855.
- [12] E. O. Hall, "The Deformation and Ageing of Mild Steel: II Characteristics of the Lüders Deformation", *Proceedings of the Physical Society Section B* **64** (1951), no. 9, p. 742-747.
- [13] R. W. Armstrong, "The influence of polycrystal grain size on several mechanical properties of materials", *Metallurgical and Materials Transactions B* **1** (1970), no. 5, p. 1169-1176.
- [14] N. J. Petch, "The cleavage strength of polycrystals", *Journal of the Iron and Steel Institute* **174** (1953), p. 25-28.
- [15] D. J. Dunstan, A. J. Bushby, "The scaling exponent in the size effect of small scale plastic deformation", *International Journal of Plasticity* **40** (2013), p. 152-162.
- [16] D. J. Dunstan, A. J. Bushby, "Grain size dependence of the strength of metals: The Hall-Petch effect does not scale as the inverse square root of grain size", *International Journal of Plasticity* **53** (2014), p. 56-65.
- [17] O. Kraft, P. A. Gruber, R. Mönig, D. Weygand, "Plasticity in Confined Dimensions", *Annual Review of Materials Research* **40** (2010), no. 1, p. 293-317.
- [18] J. A. El-Adawy, "Unravelling the physics of size-dependent dislocation-mediated plasticity", *Nature Communications* **6** (2015), no. 1, article no. 5926.
- [19] C. A. Schuh, T. Nieh, T. Yamasaki, "Hall-Petch breakdown manifested in abrasive wear resistance of nanocrystalline nickel", *Scripta Materialia* **46** (2002), no. 10, p. 735-740.
- [20] H. Van Swygenhoven, J. R. Weertman, "Deformation in nanocrystalline metals", *Materials Today* **9** (2006), no. 5, p. 24-31.
- [21] G. Saada, T. Kruml, "Deformation mechanisms of nanograined metallic polycrystals", *Acta Materialia* **59** (2011), no. 7, p. 2565-2574.
- [22] L. Lu, L. B. Wang, B. Z. Ding, K. Lu, "High-tensile ductility in nanocrystalline copper", *Journal of Materials Research* **15** (2000), no. 2, p. 270-273.
- [23] D. S. Gianola, S. V. Van Petegem, M. Legros, S. Brandstetter, H. Van Swygenhoven, K. J. Hemker, "Stress-assisted discontinuous grain growth and its effect on the deformation behavior of nanocrystalline aluminum thin films", *Acta Materialia* **54** (2006), no. 8, p. 2253-2263.
- [24] D. Farkas, A. Frøseth, H. Van Swygenhoven, "Grain boundary migration during room temperature deformation of nanocrystalline Ni", *Scripta Materialia* **55** (2006), no. 8, p. 695-698.
- [25] V. Yamakov, D. Wolf, S. R. Phillpot, A. K. Mukherjee, H. Gleiter, "Deformation-mechanism map for nanocrystalline metals by molecular-dynamics simulation", *Nature Materials* **3** (2004), no. 1, p. 43-47.
- [26] Q. Yu, M. Legros, A. M. Minor, "In situ TEM nanomechanics", *MRS Bulletin* **40** (2015), p. 62-70.
- [27] R. W. Balluffi, J. W. Cahn, "Mechanism for diffusion induced grain boundary migration", *Acta Metallurgica* **29** (1981), no. 3, p. 493-500.
- [28] M. Guillopé, J.-P. Poirier, "A model for stress-induced migration of tilt grain boundaries in crystals of NaCl structure", *Acta Metallurgica* **28** (1980), no. 2, p. 163-167.
- [29] Z. Shan, E. A. Stach, J. M. K. Wiezorek, J. A. Knapp, D. M. Follstaedt, S. X. Mao, "Grain Boundary-Mediated Plasticity in Nanocrystalline Nickel", *Science* **305** (2004), p. 654-657.
- [30] M. Chen, X. Yan, "Comment on "Grain Boundary-Mediated Plasticity in Nanocrystalline Nickel"", *Science* **308** (2005), article no. 356c.
- [31] T. J. Rupert, D. S. Gianola, Y. Gan, K. J. Hemker, "Experimental Observations of Stress-Driven Grain Boundary Migration", *Science* **326** (2009), no. 5960, p. 1686-1690.
- [32] M. Legros, D. S. Gianola, K. J. Hemker, "In situ TEM observations of fast grain-boundary motion in stressed nanocrystalline aluminum films", *Acta Materialia* **56** (2008), no. 14, p. 3380-3393.
- [33] Y. Zhang, J. A. Sharon, G. Hu, K. T. Ramesh, K. J. Hemker, "Stress-driven grain growth in ultrafine grained Mg thin film", *Scripta Materialia* **68** (2013), no. 6, p. 424-427.
- [34] K. Zhang, J. R. Weertman, J. A. Eastman, "Rapid stress-driven grain coarsening in nanocrystalline Cu at ambient and cryogenic temperatures", *Applied Physics Letters* **87** (2005), no. 6, article no. 061921.
- [35] W. T. Read, W. Shockley, "Dislocation models of crystal grain boundaries", *Physical Review* **78** (1950), no. 3, p. 275-289.
- [36] D. W. Bainbridge, C. H. Li, E. H. Edwards, "Recent observations on the motion of small angle dislocation boundaries", *Acta Metallurgica* **2** (1954), no. 2, p. 322-333.
- [37] C. H. Li, E. H. Edwards, J. Washburn, E. R. Parker, "Stress-induced movement of crystal boundaries", *Acta Metallurgica* **1** (1953), no. 2, p. 223-229.
- [38] J. Yang, Y. Nagai, M. Hasegawa, "Use of the Frank-Bilby equation for calculating misfit dislocation arrays in interfaces", *Scripta Materialia* **62** (2010), no. 7, p. 458-461.

- [39] J. W. Cahn, Y. Mishin, A. Suzuki, "Coupling grain boundary motion to shear deformation", *Acta Materialia* **54** (2006), no. 19, p. 4953-4975.
- [40] T. Gorkaya, D. A. Molodov, G. Gottstein, "Stress-driven migration of symmetrical  $\langle 100 \rangle$  tilt grain boundaries in Al bicrystals", *Acta Materialia* **57** (2009), no. 18, p. 5396-5405.
- [41] D. A. Molodov, T. Gorkaya, G. Gottstein, "Migration of the  $\Sigma 7$  tilt grain boundary in Al under an applied external stress", *Scripta Materialia* **65** (2011), no. 11, p. 990-993.
- [42] V. A. Ivanov, Y. Mishin, "Dynamics of grain boundary motion coupled to shear deformation: An analytical model and its verification by molecular dynamics", *Phys. Rev. B* **78** (2008), no. 6, article no. 064106.
- [43] F. Momprou, D. Caillard, M. Legros, "Grain boundary shear-migration coupling—I. In situ TEM straining experiments in Al polycrystals", *Acta Materialia* **57** (2009), no. 7, p. 2198-2209.
- [44] E. R. Homer, S. M. Foiles, E. A. Holm, D. L. Olmsted, "Phenomenology of shear-coupled grain boundary motion in symmetric tilt and general grain boundaries", *Acta Materialia* **61** (2013), no. 4, p. 1048-1060.
- [45] D. Caillard, F. Momprou, M. Legros, "Grain-boundary shear-migration coupling. II. Geometrical model for general boundaries", *Acta Materialia* **57** (2009), no. 8, p. 2390-2402.
- [46] G. Bradski, "The OpenCV library", *Dr Dobbs's J. Software Tools* **25** (2000), p. 120-125.
- [47] F. Momprou, M. Legros, "Quantitative grain growth and rotation probed by in-situ TEM straining and orientation mapping in small grained Al thin films", *Scripta Materialia* **99** (2015), p. 5-8.
- [48] Y. Mishin, M. J. Mehl, D. A. Papaconstantopoulos, A. F. Voter, J. D. Kress, "Structural stability and lattice defects in copper: Ab initio, tight-binding, and embedded-atom calculations", *Phys. Rev. B* **63** (2001), no. 22, article no. 224106.
- [49] S. Plimpton, "Fast Parallel Algorithms for Short-Range Molecular Dynamics", *J. Comput. Phys.* **117** (1995), no. 1, p. 1-19.
- [50] A. Rajabzadeh, "Experimental and theoretical study of the shear-coupled grain boundary migration mechanism", PhD Thesis, Université Paul Sabatier (Toulouse 3), 2013.
- [51] D. Sheppard, R. Terrell, G. Henkelman, "Optimization methods for finding minimum energy paths", *J. Chem. Phys.* **128** (2008), no. 13, article no. 134106.
- [52] H. A. Khater, A. Serra, R. C. Pond, J. P. Hirth, "The disconnection mechanism of coupled migration and shear at grain boundaries", *Acta Materialia* **60** (2012), no. 5, p. 2007-2020.
- [53] A. Rajabzadeh, F. Momprou, S. Lartigue-Korinek, N. Combe, M. Legros, D. A. Molodov, "The role of disconnections in deformation-coupled grain boundary migration", *Acta Materialia* **77** (2014), p. 223-235.
- [54] F. Momprou, M. Legros, D. Caillard, "Stress assisted grain growth in ultrafine and nanocrystalline aluminum revealed by in-situ TEM", *MRS Proceedings Online Library* **1086** (2008), article no. 10860904.
- [55] F. Momprou, M. Legros, D. Caillard, "Grain Boundary Based Plasticity: In-Situ TEM Experiments and Modelling", *Minerals, Metals and Materials Society/AIME* **57** (2011), no. 7, p. 2198-2209.
- [56] P. F. Rottmann, K. J. Hemker, "Experimental quantification of mechanically induced boundary migration in nanocrystalline copper films", *Acta Materialia VL - 140* (2017), p. 46-55.
- [57] A. Kobler, A. Kashiwar, H. H. Hahn, C. Kübel, "Combination of in situ straining and ACOM TEM: A novel method for analysis of plastic deformation of nanocrystalline metals", *Ultramicroscopy* **128** (2013), p. 68-81.
- [58] E. Izadi, A. Darbal, R. Sarkar, J. Rajagopalan, "Grain rotations in ultrafine-grained aluminum films studied using in situ TEM straining with automated crystal orientation mapping", *Materials & Design* **113** (2017), p. 186-194.
- [59] G. Gottstein, D. A. Molodov, L. S. Shvindlerman, D. J. Srolovitz, M. Winning, "Grain boundary migration: misorientation dependence", *Current Opinion in Solid State and Materials Science* **5** (2001), no. 1, p. 9-14.
- [60] K. D. Molodov, D. A. Molodov, "Grain boundary mediated plasticity: On the evaluation of grain boundary migration - shear coupling", *Acta Materialia VL - 153* (2018), p. 336-353.
- [61] R. C. Pond, W. Bollmann, "The symmetry and interfacial structure of bicrystals", *Philos. Trans. R. Soc. Lond. Ser. A Math. Phys. Eng. Sci.* **292** (1979), no. 1395, p. 449-472.
- [62] R. C. Pond, D. A. Smith, "On the absorption of dislocations by grain boundaries", *Philosophical Magazine* **36** (1977), no. 2, p. 353-366.
- [63] J. P. Hirth, R. C. Pond, "Steps, dislocations and disconnections as interface defects relating to structure and phase transformations", *Acta Materialia* **44** (1996), no. 12, p. 4749-4763.
- [64] W. A. Swiatnicki, W. Łojkowski, M. W. Grabski, "Investigation of grain boundary diffusion in polycrystals by means of extrinsic grain boundary dislocations spreading rate", *Acta Metallurgica* **34** (1986), no. 4, p. 599-605.
- [65] F. Momprou, D. Caillard, M. Legros, H. Mughrabi, "In-situ TEM observations of reverse dislocation motion upon unloading in tensile-deformed UFG aluminium", *Acta Materialia* **60** (2012), no. 8, p. 3402-3414.
- [66] R. C. Pond, S. Celotto, "Special interfaces: military transformations", *International Materials Reviews* **48** (2003), no. 4, p. 225-245.
- [67] J. M. Howe, R. C. Pond, J. P. Hirth, "The role of disconnections in phase transformations", *Progress in Materials Science* **54** (2009), no. 6, Sp. Iss. SI, p. 792-838.
- [68] J. P. Hirth, R. C. Pond, "Steps, dislocations and disconnections as interface defects relating to structure and phase transformations", *Acta Materialia* **44** (1996), no. 12, p. 4749-4763.



- [69] A. Serra, R. C. Pond, D. J. Bacon, "Computer simulation of the structure and mobility of twinning dislocations in H.C.P. Metals", *Acta Metallurgica et Materialia* **39** (1991), no. 7, p. 1469-1480.
- [70] A. Rajabzadeh, F. Momprou, M. Legros, N. Combe, "Elementary mechanisms of shear-coupled grain boundary migration", *Phys. Rev. Lett.* **110** (2013), no. 26, article no. 265507.
- [71] J. Han, S. L. Thomas, D. J. Srolovitz, "Grain-boundary kinetics: A unified approach", *Progress in Materials Science* **98** (2018), p. 386-476.
- [72] A. Serra, D. J. Bacon, "A model for simulating the motion of line defects in twin boundaries in HCP metals", *Zeitschrift für Metallkunde* **95** (2004), no. 4, p. 242-243.
- [73] K. D. Molodov, T. Al-Samman, D. A. Molodov, S. Korte-Kerzel, "On the twinning shear of  $\{101\}^2$  twins in magnesium – Experimental determination and formal description", *Acta Materialia* **134** (2017), p. 267-273.
- [74] A. Serra, N. Kvashin, N. Anento, "On the common topological conditions for shear-coupled twin boundary migration in bcc and hcp metals", *Letters on Materials* **10** (2020), no. 4s, p. 537-542.
- [75] Q. Zhu, G. Cao, J. Wang, C. Deng, J. Li, Z. Zhang, S. X. Mao, "In situ atomistic observation of disconnection-mediated grain boundary migration", *Nature Communications* **10** (2019), no. 1, article no. 156.
- [76] A. Rajabzadeh, M. Legros, N. Combe, F. Momprou, D. A. Molodov, "Evidence of grain boundary dislocation step motion associated to shear-coupled grain boundary migration", *Philosophical Magazine* **93** (2013), no. 10-12, p. 1299-1316.
- [77] K. Marukawa, Y. Matsubara, "A new method of Burgers vector identification for grain boundary dislocations from electron microscopic images", *Transactions of the Japan Institute of Metals* **20** (1979), no. 10, p. 560-568.
- [78] M. Larranaga, F. Momprou, M. Legros, N. Combe, "Role of sessile disconnection dipoles in shear-coupled grain boundary migration", *Physical Review Materials* **4** (2020), no. 12, article no. 123606.
- [79] N. Combe, F. Momprou, M. Legros, "Heterogeneous disconnection nucleation mechanisms during grain boundary migration", *Physical Review Materials* **3** (2019), no. 6, article no. 060601.
- [80] N. Combe, F. Momprou, M. Legros, "Shear-coupled grain-boundary migration dependence on normal strain/stress", *Physical Review Materials* **1** (2017), no. 3, article no. 033605.
- [81] I. Shin, E. A. Carter, "Possible origin of the discrepancy in Peierls stresses of fcc metals: First-principles simulations of dislocation mobility in aluminum", *Phys. Rev. B* **88** (2013), no. 6, article no. 064106.
- [82] T. Gorkaya, T. Burlet, D. A. Molodov, G. Gottstein, "Experimental method for true in situ measurements of shear-coupled grain boundary migration", *Scripta Materialia* **63** (2010), no. 6, p. 633-636.
- [83] N. Tsuji, Y. Ito, Y. Saito, Y. Minamino, "Strength and ductility of ultrafine grained aluminum and iron produced by ARB and annealing", *Scripta Materialia* **47** (2002), p. 893-899.
- [84] K. Chen, J. Han, S. L. Thomas, D. J. Srolovitz, "Grain boundary shear coupling is not a grain boundary property", *Acta Materialia* **167** (2019), p. 241-247.